Physics-augmented models to simulate commercial adaptive cruise control (ACC) systems

Yinglong He [a], Marcello Montanino [b, *], Konstantinos Mattas [c], Vincenzo Punzo [b], Biagio Ciuffo [c]

[a] University of Birmingham, Edgbaston, Birmingham, B15 2TT, UK
[b] University of Naples Federico II, Via Claudio, 21, 80125 Napoli, IT
[c] European Commission – Joint Research Centre., Ispra (VA), IT

Introduction

Accurate simulation of mixed traffic, including human-driven vehicles (HDVs) and automated vehicles (AVs), is crucial to the development and assessment of cooperative, connected, and automated mobility (CCAM) technologies. To reproduce driving behaviors of HDVs and AVs, car-following (CF) and adaptive cruise control (ACC) models are developed in the literature of traffic flow. Moreover, these models are augmented to capture essential but overlooked aspects, e.g., vehicle dynamics, perception/actuation delays, and acceleration capabilities. However, a systematic analysis of models augmented with those aspects at different levels of detail is still lacking. This study, therefore, compares the accuracy and robustness of 90 different models, resulting from all possible combinations of five base CF/ACC models and different physics extensions, including vehicle dynamics, acceleration constraints, and perception delay.

Problem description

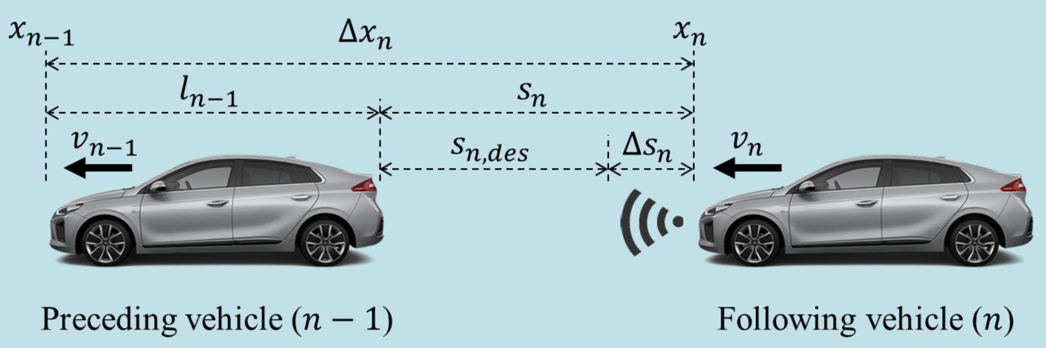

$$\begin{cases} \dot{v}_n(t) = a_n(t), \\ \dot{x}_n(t) = v_n(t), \\ s_n(t) = x_{n-1}(t) - x_n(t) - l_{n-1}, \\ \Delta v_n(t) = v_{n-1}(t) - v_n(t), \end{cases} \tag{1}$$

Fig. 1. Kinematics in car-following problems.

The movement of the following vehicle (n) depends not only on the trajectory of the preceding vehicle $(n-1)$, but also on the characteristics of the follower vehicle, driver/ACC, road, etc. In car-following problems, main variables include acceleration (a), speed (v), position (x), and inter-vehicle spacing (s).

Modelling framework

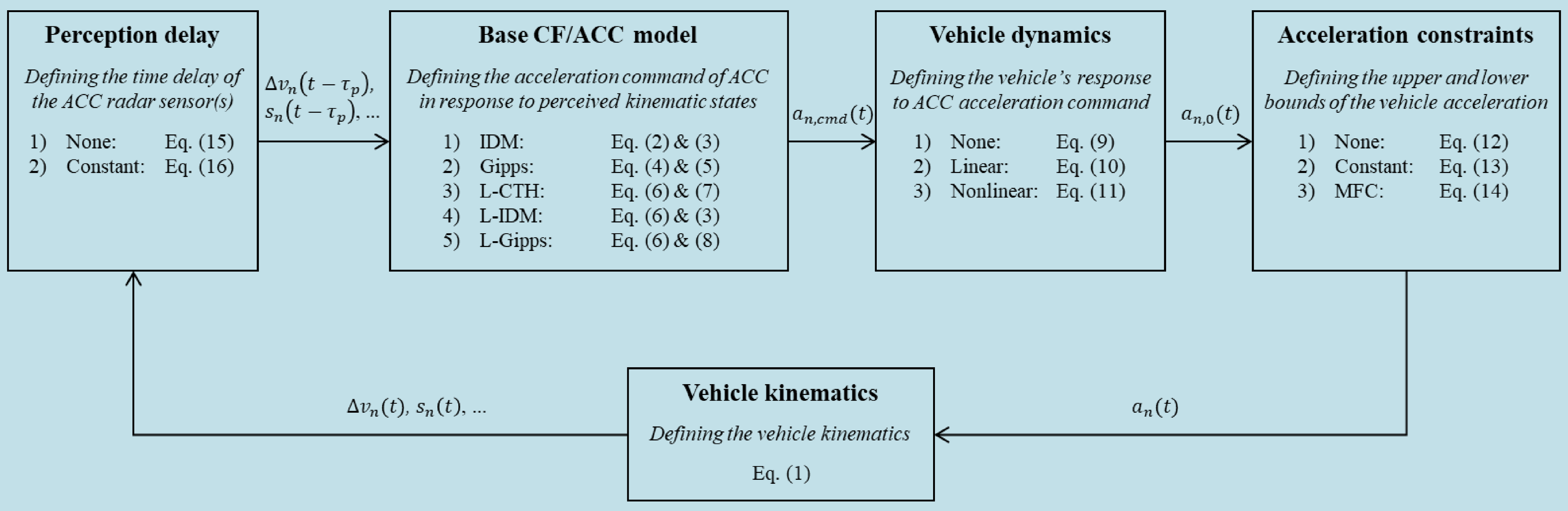

Fig. 2. Unified modelling framework.

I. Base CF/ACC models

1) Intelligent driver model (IDM):

$$a_{n,cmd}(t) = a_{max} \cdot \left(1 - \left(\frac{v_n(t)}{v_0}\right)^{\delta} - \left(\frac{s_{n,des}(t)}{s_n(t)}\right)^2\right), \tag{2}$$

IDM-desired spacing policy:

$$s_{n,des}(t) = s_0 + \max\left[0, t_h v_n(t) - \frac{v_n(t)\Delta v_n(t)}{2\sqrt{-a_{max} \cdot a_{min}}}\right], \tag{3}$$

2) Gipps' model:

$$a_{n,cmd}(t) = (v_{n,cmd}(t+t_h) - v_n(t))/t_h, \tag{4}$$

$$v_{n,cmd}(t+t_h) = \min\left\{ v_n(t) + 2.5 a_{max} t_h \cdot \left(1 - \frac{v_n(t)}{v_0}\right)\left(0.025 + \frac{v_n(t)}{v_0}\right)^{0.5}, \right.$$
$$\left. a_{min} \cdot \left(\frac{t_h}{2} + \theta\right) + \sqrt{{a_{min}}^2 \cdot \left(\frac{t_h}{2} + \theta\right)^2 - a_{min} \cdot \left(2(s_n(t) - s_0) - t_h v_n(t) - \frac{v_{n-1}(t)^2}{\hat{a}_{min}}\right)} \right\}, \tag{5}$$

3) Linear ACC models (L-CTH, L-IDM, and L-Gipps):

$$\begin{cases} a_{n,cmd}(t) = \min\left[k_v \cdot \Delta v_n(t) + k_s \cdot \Delta s_n(t), k_0 \cdot (v_0 - v_n(t))\right], \\ \Delta s_n(t) = s_n(t) - s_{n,des}(t), \end{cases} \tag{6}$$

Constant time headway (CTH) spacing policy:

$$s_{n,des}(t) = s_0 + t_h \cdot v_n(t), \tag{7}$$

Gipps-equilibrium spacing policy:

$$s_{n,des}(t) = s_0 + (t_h + \theta) v_n(t) - 0.5 v_n(t)^2 \left(\frac{1}{a_{min}} - \frac{1}{\hat{a}_{min}}\right), \tag{8}$$

II. Physics extensions

❑ Vehicle dynamics (VD)

1) None:

$$a_{n,0}(t) = a_{n,cmd}(t), \tag{9}$$

2) Linear (LVD):

$$\tau_a \cdot \dot{a}_{n,0}(t) + a_{n,0}(t) = a_{n,cmd}(t), \tag{10}$$

3) Nonlinear (NLVD):

$$\begin{cases} a_{n,0}(t) = \frac{F_t(t) - F_r(t)}{\phi \cdot m}, \\ F_r(t) = f_0 \cdot \cos\alpha(t) + f_1 \cdot v_n(t) + f_2 \cdot v_n(t)^2 + mg \cdot \sin\alpha(t), \\ F_t(t) = \frac{T_t(t)}{r_w} = m \cdot a_t(t), \\ \tau_a \cdot \dot{a}_t(t) + a_t(t) = a_{n,cmd}(t), \end{cases} \tag{11}$$

❑ Acceleration constraints (AC)

1) None:

$$a_n(t) = a_{n,0}(t), \tag{12}$$

2) Constant:

$$a_n(t) = \max\left\{a_{lb}, \min[a_{n,0}(t), a_{ub}]\right\}, \tag{13}$$

3) Microsimulation free-flow acceleration (MFC) boundary model:

$$a_n(t) = \max\left\{a_{dp}(v_n(t)), \min\left[a_{n,0}(t), a_{ap}(v_n(t))\right]\right\}, \tag{14}$$

❑ Perception delay (PD)

1) None:

$$\tau_p = 0, \tag{15}$$

2) Constant:

$$\tau_p > 0, \tag{16}$$

III. Summary of 90 models

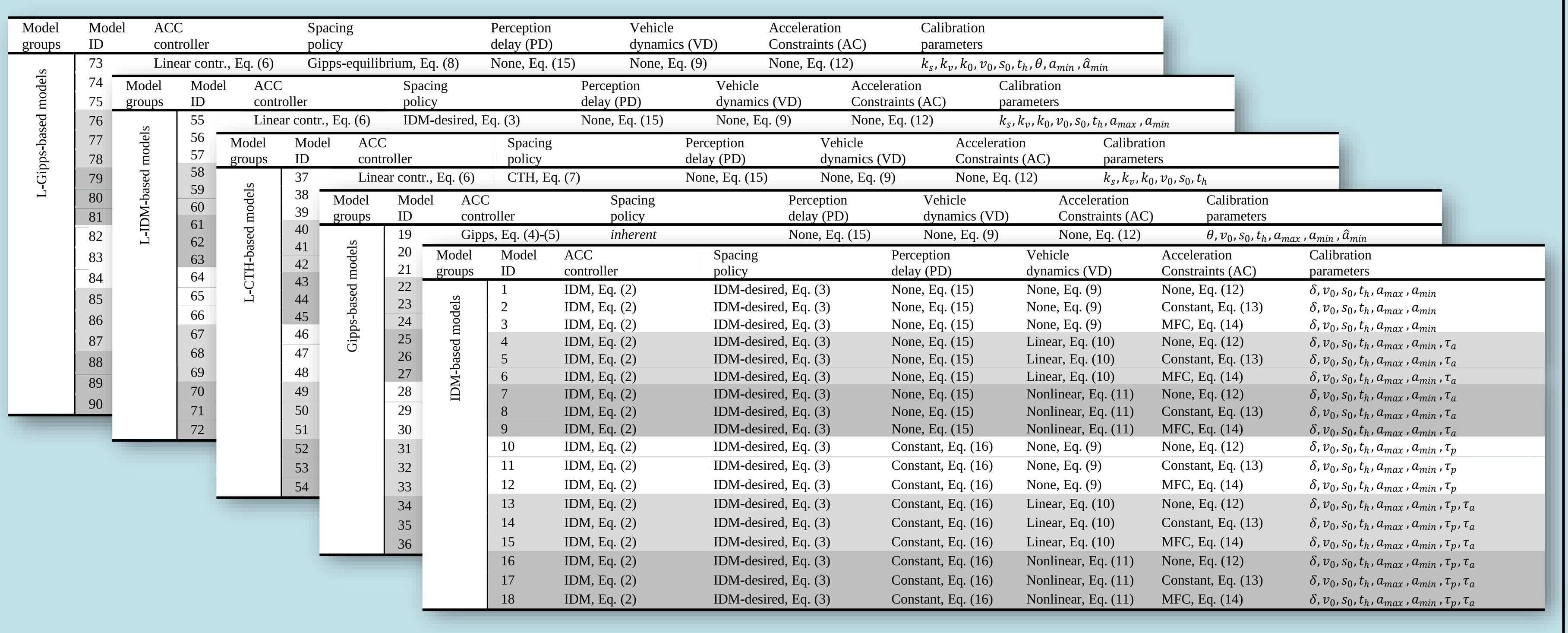

Fig. 3. Overview of Formulas and calibration parameters of 90 models.

The European Commission's science and knowledge service
Joint Research Centre

EU Science Hub: ec.europa.eu/jrc @EU_ScienceHub EU Science Hub
EU Science Hub - Joint Research Centre EU Science, Research and Innovation

This research was partially funded by the Italian program PON AIM - Attraction and International Mobility, Linea 1 (AIM1849341-2, CUP E61G18000540007).

All the data used are part of the JRC OpenACC database openly available online.

Joint Research Centre

Platoon trajectories in JRC OpenACC database

The test platoon was composed of five high-end vehicles equipped with commercial ACC. All the data used are part of the JRC OpenACC database openly available online.

Table 1. Composition of platoons.

Vehicle position	P1	P2	P3	P4	P5	P6	P7
Leader	Audi A8	Audi A8	Audi A8	Audi A8	Audi A8	Audi A8	Audi A8
Follower 1	Audi A6	Audi A6	Tesla	Tesla	Tesla	Mercedes	Mercedes
Follower 2	BMW	BMW	BMW	BMW	BMW	BMW	BMW
Follower 3	Mercedes	Mercedes	Audi A6	Audi A6	Audi A6	Tesla	Tesla
Follower 4	Tesla	Tesla	Mercedes	Mercedes	Mercedes	Audi A6	Audi A6

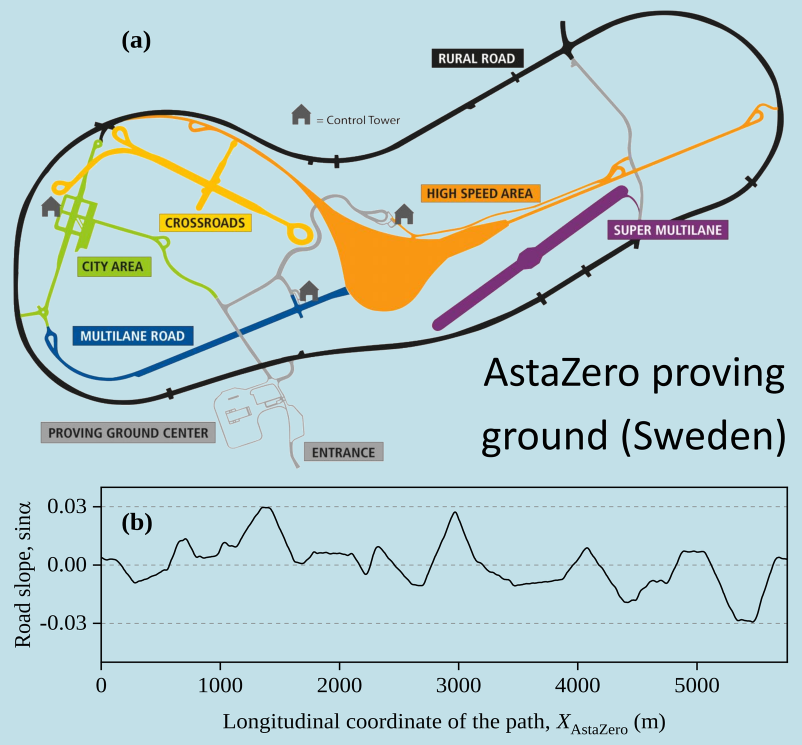

Fig. 4. Layout (a) and slope (b) of the test track.

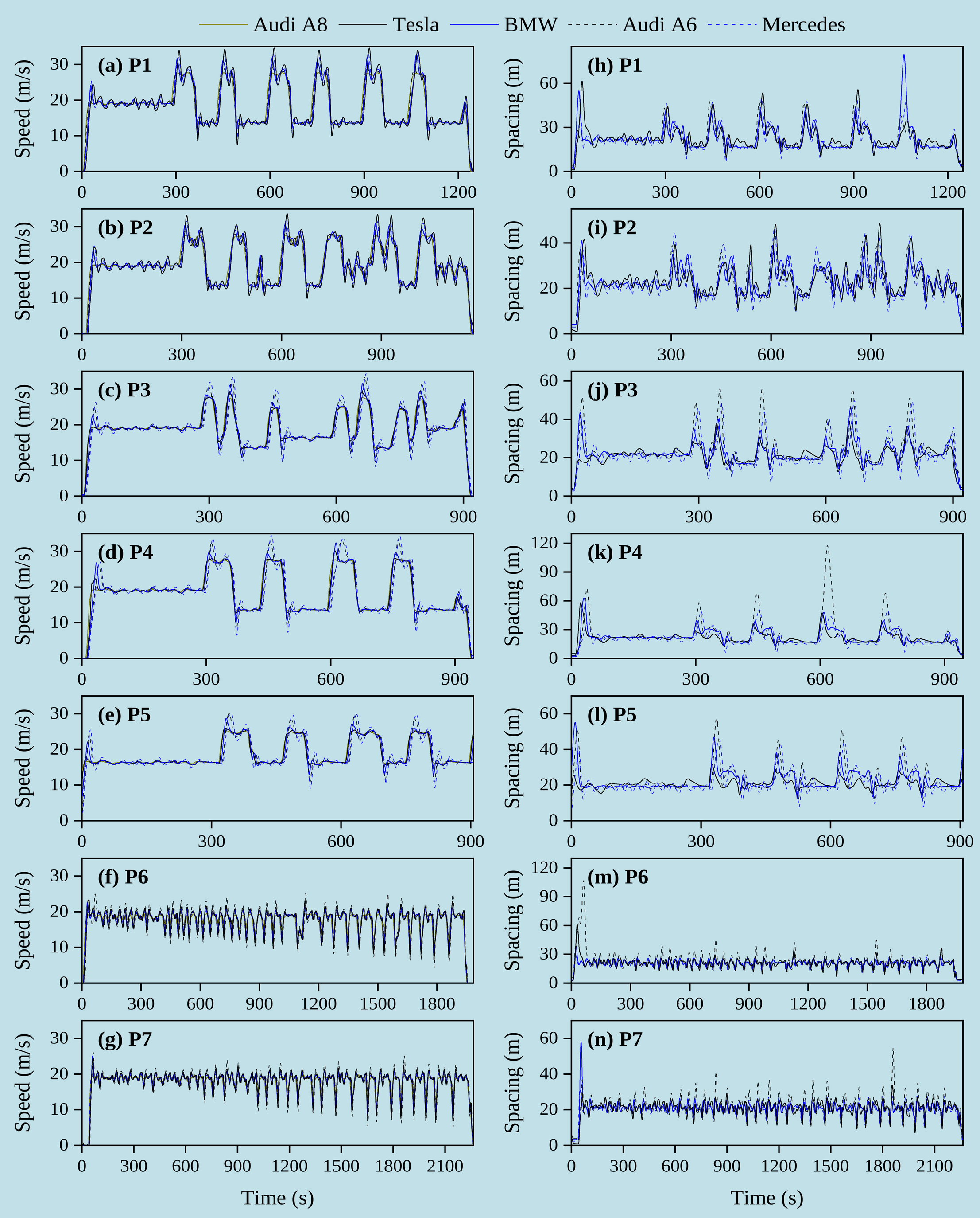

Fig. 5. Speed (left) and inter-vehicle spacing (right).

Results

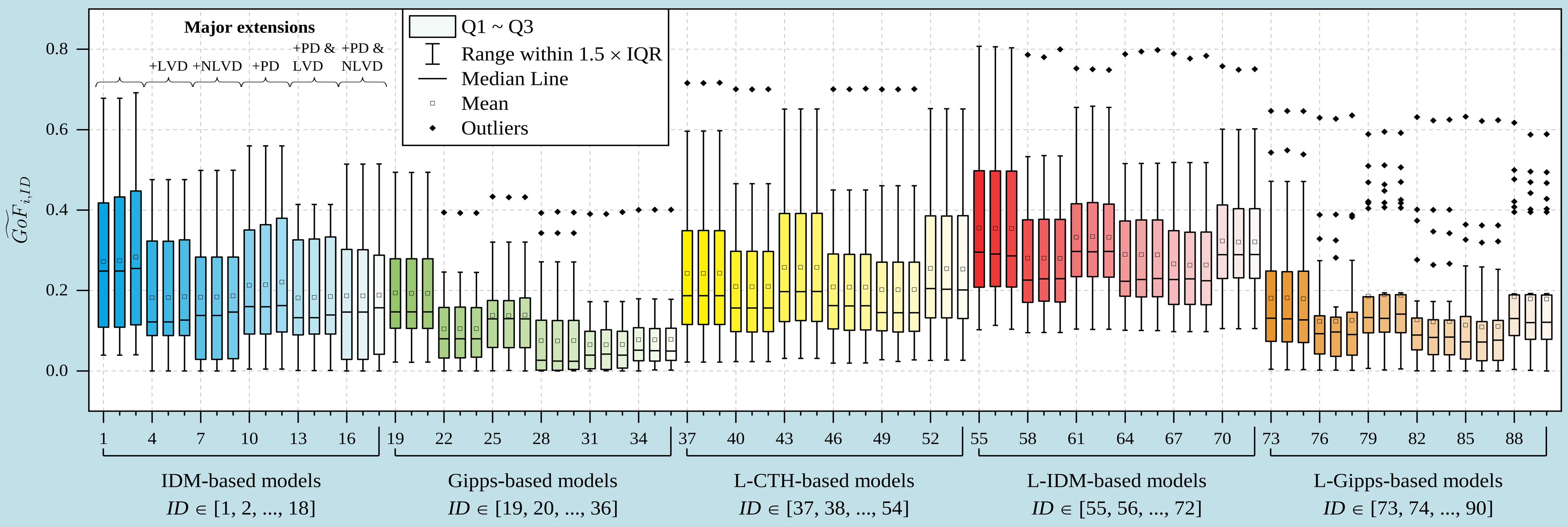

Note: GoF_i = goodness-of-fit function value for the *i*-th trajectory, calculated by NRMSE(*s*, *v*, *a*); IDM = intelligent driver model; L-CTH, L-IDM, and L-Gipps = linear models with the spacing policies of constant-time-headway (CTH), IDM-desired, and Gipps-equilibrium, respectively; IQR = interquartile range.

$$\widetilde{GoF}_{i,ID} = \frac{GoF_{i,ID} - GoF_{i,min}}{GoF_{i,min}} \text{ and } GoF_{i,min} = \min_{ID=1,\dots,90} GoF_{i,ID},$$
for $i \in [1,\dots,28]$ (trajectories) and $ID \in [1,\dots,90]$ (models)

Fig. 6. Variability of normalized calibration errors ($\widetilde{GoF}_{i,ID}$) within (individual box plot) and among models

- Variance-based sensitivity analysis: $S_{trajectories} = 0.819 > S_{models} = 0.062$.
- Gipps-based models demonstrate the best performance in calibration experiments.
- Perception delay (PD) and linear vehicle dynamics (LVD) can improve model accuracy.
- Nonlinear vehicle dynamics (NLVD) can provide accuracy benefit to IDM- and Gipps-based models.

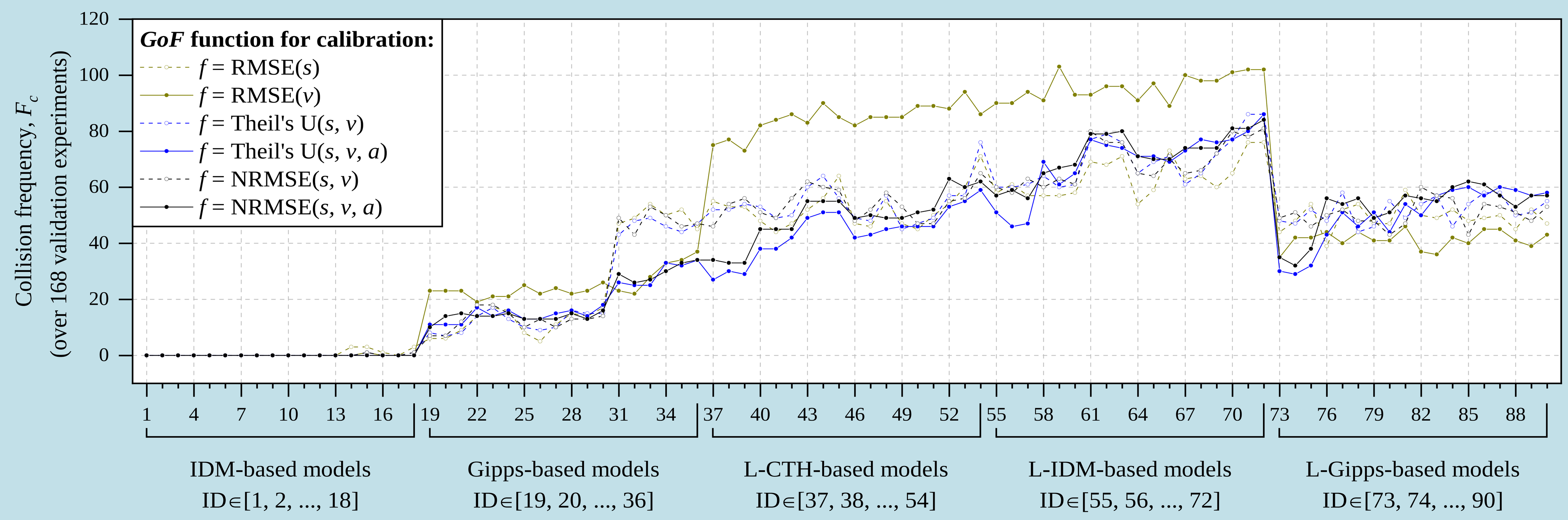

Fig. 7. Collision frequency (for each model variant) over 168 validation experiments.

- $NRMSE(s, v, a)$ and Theil's $U(s, v, a)$ lead to the least number of collisions in validation tests.
- IDM-based models outperform others regarding transferability of parameters and model robustness.

Design of experiments

I. Optimization problem

$$\begin{aligned} &\min_{\beta} f\left(Y^{obs}, Y^{sim}(\beta)\right), \\ &Y^{sim}(\beta) = F(\beta), \\ &LB_\beta \le \beta \le UB_\beta, \mathbf{G}(\beta) \le 0, \end{aligned} \tag{17}$$

β is the set of calibration parameters; F is the model; LB, UB, and $\mathbf{G}$ are constraints.

II. Evaluation metric

Goodness-of-fit (*GoF*) function: $f = \mathrm{NRMSE}(Y)$,

Measure of performance (*MoP*): $Y \in [s, v, a]$,

$$\begin{cases} \mathrm{NRMSE}(s,v,a) = w_0\mathrm{NRMSE}(s) + w_1\mathrm{NRMSE}(v) + w_2\mathrm{NRMSE}(a), \\ \mathrm{NRMSE}(Y) = \mathrm{RMSE}(Y)/\sqrt{\frac{1}{N}\sum_{i=1}^{N}\left(Y_i^{obs}\right)^2}, \\ \mathrm{RMSE}(Y) = \sqrt{\frac{1}{N}\sum_{i=1}^{N}\left(Y_i^{sim} - Y_i^{obs}\right)^2}, \end{cases} \tag{18}$$

Table 2. Bounds of calibration parameters.

Parameter [unit]	Lower bound (LB)	Upper bound (UB)
δ	0.1	10
v_0[m/s]	30	35
s_0 [m]	1	5
t_h [s]	0.1	3
a_{max} [m/s^2]	0.5	5
a_{min} [m/s^2]	-5	-0.5
$\hat{a}_{min}$ [m/s^2]	-5	-0.5
θ [s]	0	3
τ_a [s]	0.3	0.8
τ_p [s]	0.1	0.8
k_s [s^{-2}]	0.01	5
k_v [s^{-1}]	0.01	5
k_0 [s^{-1}]	0.01	5

Conclusions

I. Contributions

- A comparison framework was proposed to assess CF/ACC models augmented at different levels of detail with vehicle dynamics, acceleration constraints, and perception delay. These physics extensions were essential aspects of human/automated driving behavior.
- Two new spacing policies derived from microscopic traffic flow theory (TFT) were coupled with linear ACC controllers.
- Calibration experiments help to assess the contribution of each physics extension to the accuracy of the base model.

II. Conclusions

- Across all 90 model variants, Gipps-based models demonstrate the best performance in reproducing ACC driving trajectories.
- In terms of transferability of parameters and model robustness to vehicle collisions in validation experiments, IDM-based models outperform all other models, followed by Gipps-based ones.
- The objective (or GoF) function of $NRMSE(s, v, a)$ can sensibly improve model robustness and transferability of calibrated parameters.
- Perception delay (PD) and linear vehicle dynamics (LVD) can largely improve model accuracy.
- Nonlinear vehicle dynamics (NLVD) can provide accuracy benefit to IDM- and Gipps-based models.

This research was partially funded by the Italian program PON AIM - Attraction and International Mobility, Linea 1 (AIM1849341-2, CUP E61G18000540007).

All the data used are part of the JRC OpenACC database openly available online.